CLEO CONF 04-3
ICHEP04 ABS8-0781

First CLEO-c Results on Exclusive D^0 Semileptonic Decays *

K. Y. Gao,[1] D. T. Gong,[1] Y. Kubota,[1] B.W. Lang,[1] S. Z. Li,[1] R. Poling,[1] A. W. Scott,[1] A. Smith,[1] C. J. Stepaniak,[1] J. Urheim,[1] Z. Metreveli,[2] K. K. Seth,[2] A. Tomaradze,[2] P. Zweber,[2] J. Ernst,[3] A. H. Mahmood,[3] H. Severini,[4] D. M. Asner,[5] S. A. Dytman,[5] S. Mehrabyan,[5] J. A. Mueller,[5] V. Savinov,[5] Z. Li,[6] A. Lopez,[6] H. Mendez,[6] J. Ramirez,[6] G. S. Huang,[7] D. H. Miller,[7] V. Pavlunin,[7] B. Sanghi,[7] E. I. Shibata,[7] I. P. J. Shipsey,[7] G. S. Adams,[8] M. Chasse,[8] M. Cravey,[8] J. P. Cummings,[8] I. Danko,[8] J. Napolitano,[8] D. Cronin-Hennessy,[9] C. S. Park,[9] W. Park,[9] J. B. Thayer,[9] E. H. Thorndike,[9] T. E. Coan,[10] Y. S. Gao,[10] F. Liu,[10] M. Artuso,[11] C. Boulahouache,[11] S. Blusk,[11] J. Butt,[11] E. Dambasuren,[11] O. Dorjkhaidav,[11] N. Menaa,[11] R. Mountain,[11] H. Muramatsu,[11] R. Nandakumar,[11] R. Redjimi,[11] R. Sia,[11] T. Skwarnicki,[11] S. Stone,[11] J. C. Wang,[11] K. Zhang,[11] S. E. Csorna,[12] G. Bonvicini,[13] D. Cinabro,[13] M. Dubrovin,[13] R. A. Briere,[14] G. P. Chen,[14] T. Ferguson,[14] G. Tatishvili,[14] H. Vogel,[14] M. E. Watkins,[14] N. E. Adam,[15] J. P. Alexander,[15] K. Berkelman,[15] D. G. Cassel,[15] J. E. Duboscq,[15] K. M. Ecklund,[15] R. Ehrlich,[15] L. Fields,[15] L. Gibbons,[15] B. Gittelman,[15] R. Gray,[15] S. W. Gray,[15] D. L. Hartill,[15] B. K. Heltsley,[15] D. Hertz,[15] L. Hsu,[15] C. D. Jones,[15] J. Kandaswamy,[15] D. L. Kreinick,[15] V. E. Kuznetsov,[15] H. Mahlke-Krüger,[15] T. O. Meyer,[15] P. U. E. Onyisi,[15] J. R. Patterson,[15] D. Peterson,[15] J. Pivarski,[15] D. Riley,[15] J. L. Rosner,[15,†] A. Ryd,[15] A. J. Sadoff,[15] H. Schwarthoff,[15] M. R. Shepherd,[15] W. M. Sun,[15] J. G. Thayer,[15] D. Urner,[15] T. Wilksen,[15] M. Weinberger,[15] S. B. Athar,[16] P. Avery,[16] L. Breva-Newell,[16] R. Patel,[16] V. Potlia,[16] H. Stoeck,[16] J. Yelton,[16] P. Rubin,[17] B. I. Eisenstein,[18] G. D. Gollin,[18] I. Karliner,[18] D. Kim,[18] N. Lowrey,[18] P. Naik,[18] C. Sedlack,[18] M. Selen,[18] J. J. Thaler,[18] J. Williams,[18] J. Wiss,[18] K. W. Edwards,[19] and D. Besson[20]

(CLEO Collaboration)

[1] *University of Minnesota, Minneapolis, Minnesota 55455*
[2] *Northwestern University, Evanston, Illinois 60208*
[3] *State University of New York at Albany, Albany, New York 12222*
[4] *University of Oklahoma, Norman, Oklahoma 73019*
[5] *University of Pittsburgh, Pittsburgh, Pennsylvania 15260*
[6] *University of Puerto Rico, Mayaguez, Puerto Rico 00681*
[7] *Purdue University, West Lafayette, Indiana 47907*
[8] *Rensselaer Polytechnic Institute, Troy, New York 12180*
[9] *University of Rochester, Rochester, New York 14627*
[10] *Southern Methodist University, Dallas, Texas 75275*
[11] *Syracuse University, Syracuse, New York 13244*
[12] *Vanderbilt University, Nashville, Tennessee 37235*
[13] *Wayne State University, Detroit, Michigan 48202*
[14] *Carnegie Mellon University, Pittsburgh, Pennsylvania 15213*
[15] *Cornell University, Ithaca, New York 14853*
[16] *University of Florida, Gainesville, Florida 32611*
[17] *George Mason University, Fairfax, Virginia 22030*
[18] *University of Illinois, Urbana-Champaign, Illinois 61801*
[19] *Carleton University, Ottawa, Ontario, Canada K1S 5B6*

and the Institute of Particle Physics, Canada
[20]*University of Kansas, Lawrence, Kansas 66045*
(Dated: February 7, 2008)

Abstract

Based on a data sample of 60 pb^{-1} collected at the $\psi(3770)$ resonance with the CLEO-c detector at CESR, we present improved measurements of absolute branching fractions for exclusive D^0 semileptonic decays into $K^-e^+\nu$, $\pi^-e^+\nu$ and $K^{*-}e^+\nu$; and the first observation and absolute branching fraction measurement of $D^0 \to \rho^-e^+\nu$.

*Submitted to the 32nd International Conference on High Energy Physics, Aug 2004, Beijing
†On leave of absence from University of Chicago.

I. INTRODUCTION

The quark mixing parameters in the Cabibbo-Kobayashi-Maskawa (CKM) matrix are fundamental constants that must be determined from experiments. Semileptonic D meson decays are of great physics interest because they are relatively simple to handle theoretically. The decay matrix for semileptonic D meson decay decouples into a weak current (describing the $W\ell\nu$ vertex), and a strong current (for the $Wc\bar{q}$ vertex) that is parameterized through form-factor functions of the invariant mass (q^2) of the W exchanged. The form factors can not be easily computed in quantum chromodynamics (QCD) since they are affected by significant nonperturbative contributions. That is the main source of uncertainty in the extraction of the CKM matrix element from the simple decay processes. Precise experimental measurements are needed to guide theoretical progress in this area. Charm semileptonic decays allow measurements of the form factors and CKM matrix elements V_{cs} and V_{cd}. Using Heavy Quark Effective Theory (HQET) or lattice gauge techniques, the measured charm form factors can be related to those needed to interpret $b \to u$ transition and the measurement of the CKM matrix element V_{ub}.

While measurements of form factors in all charm exclusive semileptonic decays are important, those in pseudoscalar-to-pseudoscalar transitions are the easiest to perform. The differential decay rate for the exclusive semileptonic decay $D \to P\ell\nu$ (P stands for a pseudoscalar meson) with the electron mass effects neglected can be expressed as [1]:

$$\frac{d\Gamma}{dq^2} = \frac{G_F^2}{24\pi^3} \left|V_{cq'}\right|^2 p_P^3 \left|f_+(q^2)\right|^2 \tag{1}$$

where G_F is the Fermi coupling constant, q^2 is the four-momentum transfer squared between the parent D meson and the final state meson, p_P is the momentum of the pseudoscalar meson in the D rest frame, and $V_{cq'}$ is the relevant CKM matrix element, either V_{cs} or V_{cd}. $f_+(q^2)$ is the form factor that measures the probability that the flavor changed quark q' and the spectator quark $\bar{q}$ in Fig. 1 will form a meson in the final state. The corresponding branching fractions can be obtained from

$$\mathcal{B}(D \to P\ell\nu) = \tau_D \times \int_{q^2} dq^2 \frac{d\Gamma}{dq^2} \tag{2}$$

II. DETECTOR AND DATA SET

The data sample used in this analysis was produced at the $\psi(3770)$ resonance with the Cornell Electron Storage Ring (CESR) and collected with the general purpose CLEO-c detector [2, 3]. The total integrated luminosity of this data set is 60 pb^{-1}.

The CLEO-c tracking system covers about 95% of the 4π solid angle with a large cylindrical drift chamber and an all stereo wire vertex chamber. These tracking devices also provide specific-ionization (dE/dx) measurements for particle identification. The electromagnetic calorimeter is made of 7800 cesium iodide crystals with a total solid-angle coverage of 95% of 4π. The calorimeter is crucial for electron identification and provides excellent efficiency and energy resolution for photons, yielding a typical mass resolution for π^0 reconstruction around 6 MeV/c^2 (standard deviation). The Ring Imaging Cherenkov (RICH) detector covers 80% of the 4π solid angle and provides superb particle identification capability.

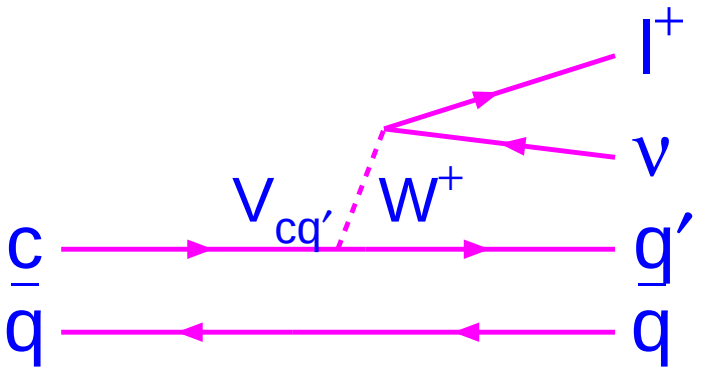

FIG. 1: Feynman diagram for charm meson semileptonic decays.

III. EVENT RECONSTRUCTION AND SELECTION

For this analysis we take full advantage of the unique kinematics of $D\bar{D}$ production at the $\psi(3770)$ resonance, just above charm threshold. We first select events in which a D^0 meson is fully reconstructed in one of the nine hadronic final states: $K^-\pi^+$, $K^-\pi^+\pi^0$, $K^-\pi^+\pi^0\pi^0$, $K^-\pi^+\pi^+\pi^-$, $K_S\pi^0$, $K_S\pi^+\pi^-$, $K_S\pi^+\pi^-\pi^0$, $\pi^+\pi^-\pi^0$, and K^-K^+. Charge conjugation is implied here and throughout this paper. Within these tagged events we select the subset in which the $\bar{D}^0$ meson decayed semileptonically to a specific final state. The efficiency-corrected ratio of the event yields gives the absolute branching fraction for the exclusive semileptonic decay mode. This branching fraction is independent of the luminosity of the experiment and benefits from the cancellation of many systematic uncertainties. This selection procedure provides an exceptionally clean sample of semileptonic decays that is ideal for determination of form-factor parameters and CKM elements, although our current data sample is not yet adequate for these determinations.

Full details of the hadronic event reconstruction and tag selection can be found in a separate paper [4]. The selection is based on two variables. ΔE is the difference between the beam energy and the energy of the fully reconstructed D^0 candidate. M_D is the beam-constrained mass of the D^0 candidate, which is defined as $M_D \equiv \sqrt{E_b^2 - |p_D|^2}$, where E_b is the beam energy and p_D is the measured momentum of the D^0 candidate. Fits to the beam-constrained mass distributions for D^0 candidates are shown in Fig. 2. Multiple combinations have been eliminated by selecting the candidate with the minimum value of $|\Delta E|$. The signal component in these fits consists of a Gaussian and a bifurcated Gaussian, which is found to adequately describe initial-state radiation (ISR). The background component in these fits is presented by an Argus function [5]. The tag yields and efficiencies for selecting tags are given in Table I.

The fully reconstructed D^0 meson serves as a tag and results in great suppression of backgrounds. We then identify an electron and a set of hadrons recoiling against the tag, to reconstruct the semileptonic decay side of the $D^0\bar{D}^0$ system. Electron candidates are required to have $|\cos\theta| < 0.9$, where θ is the angle between the electron direction and the beam axis, with momenta greater than 200 MeV, the minimum to reach the CsI calorimeter

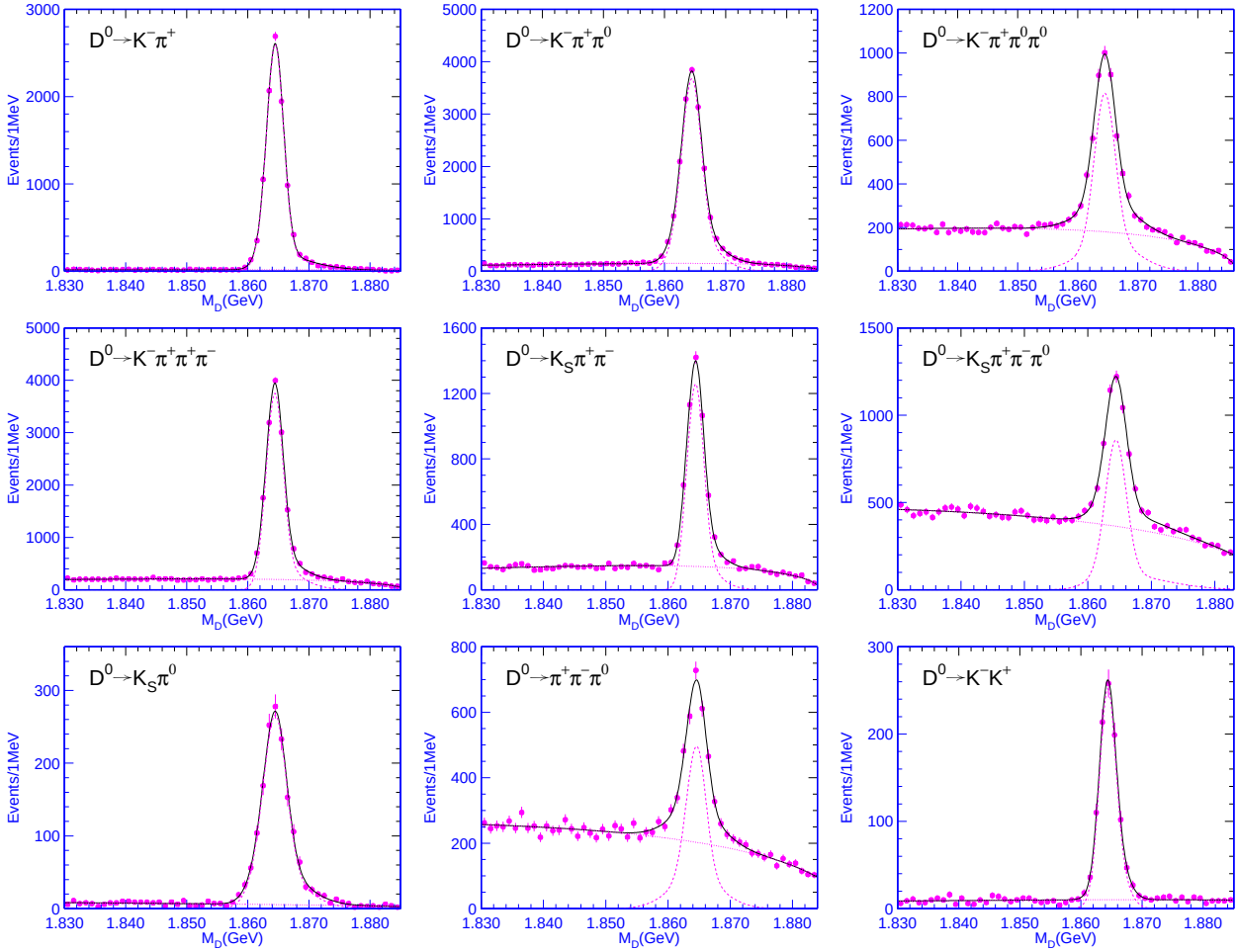

FIG. 2: Fits to the beam-constrained masses for different fully reconstructed D^0 decay modes. The signal is described by a Gaussian and a bifurcated Gaussian to account for the initial state radiation. The background is described by an Argus function [5].

TABLE I: The tag yields, efficiencies, and signal yields and efficiencies for $D^0 \to K^- e^+ \nu$.

Tags: $D^0 \to$	tag yields	$\epsilon_{\rm tag}$	signal yields	$\epsilon_{\rm signal}$	$\mathcal{B}(\%)$
$K^-\pi^+$	10183±112	(65.35±0.12)%	245.7±15.3	(42.69±0.21)%	3.69±0.23
$K^-\pi^+\pi^0$	17208±160	(33.53±0.07)%	407.7±20.4	(22.07±0.18)%	3.60±0.18
$K^-\pi^+\pi^0\pi^0$	4475±208	(16.10±0.06)%	106.6±10.6	(10.86±0.13)%	3.53±0.39
$K^-\pi^+\pi^+\pi^-$	14515±162	(46.93±0.09)%	310.3±18.0	(29.80±0.20)%	3.37±0.20
$K_S\pi^+\pi^-$	4629±101	(37.05±0.15)%	100.0±10.2	(24.25±0.19)%	3.30±0.34
$K_S\pi^+\pi^-\pi^0$	4403±240	(18.51±0.09)%	119.2±10.6	(12.83±0.19)%	3.91±0.41
$K_S\pi^0$	1502±43	(27.92±0.22)%	26.6±5.3	(19.19±0.17)%	2.58±0.52
$\pi^-\pi^+\pi^0$	2533±176	(39.91±0.19)%	63.3±8.0	(26.67±0.19)%	3.74±0.54
K^-K^+	928±35	(56.08±0.38)%	22.4±4.9	(37.04±0.21)%	3.66±0.81
all tags			1405.1±38.5	weighted ave.	3.52±0.10

for energy measurement. Electron candidates are selected with criteria that rely mostly on the ratio of the energy deposited in the CsI calorimeter to the measured momentum (E/p), dE/dx and RICH information. Extensive studies of efficiencies and misidentification rates have been performed using CLEO-c data for this electron identification procedure. Charged pions and kaons are identified using dE/dx and RICH information. For charged tracks with momenta less than 0.6 GeV, consistent dE/dx information (within 3 standard deviation (σ)) is required for pion or kaon candidates. For charged tracks with momenta greater than 0.6 GeV, additional requirement on RICH, if available, is imposed for pion or kaon candidates. K^- and π^0 candidates are combined to form K^{*-} candidates in $D^0 \to K^{*-}e^+\nu$ decays. We require the invariant masses of the K^{*-} candidates to be within 100 MeV of the K^{*-} nominal mass [6]. In case of multiple K^{*-} candidates, we select the candidate whose mass is closest to the K^{*-} nominal mass. π^- and π^0 candidates are combined to form ρ^- candidates in $D^0 \to \rho^- e^+\nu$ decays. We require the invariant masses of the ρ^- candidates to be within 150 MeV of the ρ^- nominal mass [6]. In case of multiple ρ^- candidates, we select the candidate whose mass is closest to the ρ^- nominal mass. We reconstruct exclusive D^0 semileptonic decays into $K^-e^+\nu$, $\pi^-e^+\nu$, $K^{*-}e^+\nu$ and $\rho^-e^+\nu$. No additional charged track is allowed to exist, besides those of the tagged D^0 and the semileptonic side of the other $\bar{D}^0$. The excellent particle identification of the CLEO-c detector helps in this reconstruction. The unique kinematics of threshold production provide additional and very powerful means to reject background from misidentified and missing particles. The difference between the missing energy and missing momentum in a event, $U = E_{\rm miss} - p_{\rm miss}$, would peak at zero if the event is correctly reconstructed due to the undetected neutrino.

In Fig. 3, we present kaon momentum versus U for signal $D^0 \to K^-e^+\nu$ and the background from $D^0 \to \pi^-e^+\nu$ reconstructed as $D^0 \to K^-e^+\nu$ without hadron identification using MC simulation. It clear that the $D^0 \to K^-e^+\nu$ signal and $D^0 \to \pi^-e^+\nu$ background are well-separated even without kaon identification, thanks to the kinematics of threshold production. The separation decreases as the kaon momentum increases.

Similarly, in Fig. 4, we present pion momentum versus U for signal $D^0 \to \pi^-e^+\nu$ and the background from $D^0 \to K^-e^+\nu$ reconstructed as $D^0 \to \pi^-e^+\nu$ without hadron identification. Again, the signal and the dominant background are well-separated. Therefore, tight hadron identification is not necessary for the semileptonic decay (signal) side.

IV. RESULTS

The absolute branching fractions of D^0 semileptonic decay is given by

$$\mathcal{B} = \frac{N_{\rm signal}/\epsilon_{\rm signal}}{N_{\rm tag}/\epsilon_{\rm tag}}. \tag{3}$$

$N_{\rm signal}$ is the number of the $D^0\bar{D}^0$ events with one D^0 fully reconstructed and the other $\bar{D}^0$ reconstructed through its corresponding exclusive semileptonic decay mode. ϵ_{signal} is the efficiency for constructing the fully reconstructed (tag) D^0 and the exclusive semileptonic decay of the $\bar{D}^0$. Similarly, $N_{\rm tag}$ is the number of the fully reconstructed (tag) D^0 events observed, and ϵ_{tag} is the efficiency for fully reconstructing the D^0. Therefore, $\epsilon_{signal}/\epsilon_{tag}$ is the efficiency for reconstructing the exclusive D^0 semileptonic decay in the presence of a found $\bar{D}^0$ tag.

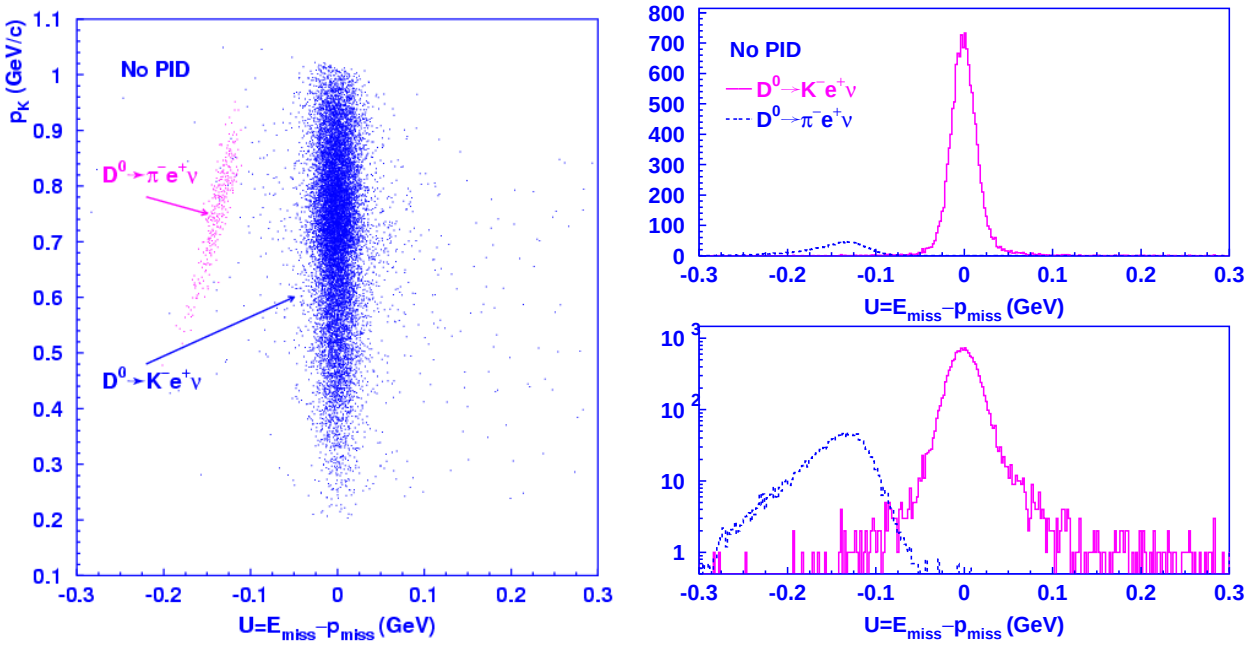

FIG. 3: Kaon momentum vs. $U = E_{\rm miss} - p_{\rm miss}$ from $D^0 \to K^- e^+ \nu$ signal MC. The background from $D^0 \to \pi^- e^+ \nu$ reconstructed as $D^0 \to K^- e^+ \nu$ is overlaid and normalized by $\frac{\mathcal{B}(D^0 \to \pi^- e^+ \nu)}{\mathcal{B}(D^0 \to K^- e^+ \nu)} = 0.1$ from PDG [6]. The right plot shows the projection onto the U axis in linear and log scales.

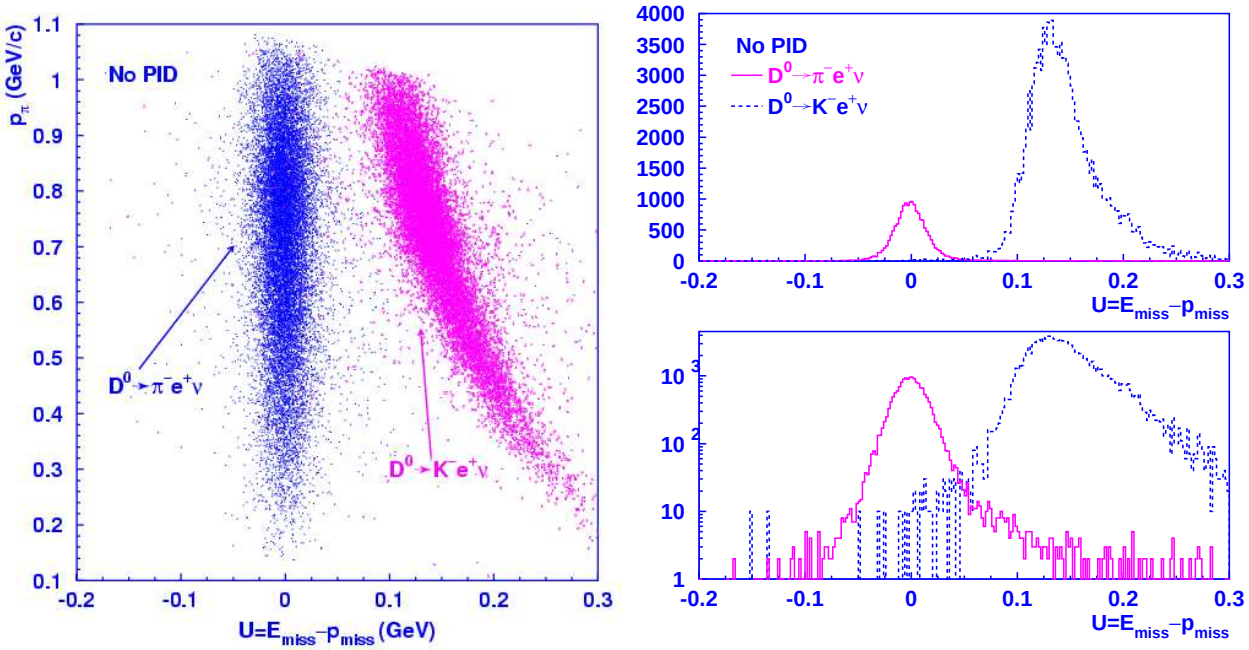

FIG. 4: Pion momentum vs. $U = E_{miss} - p_{miss}$ from $D^0 \to \pi^- e^+ \nu$ signal MC. The background from $D^0 \to K^- e^+ \nu$ reconstructed as $D^0 \to \pi^- e^+ \nu$ is overlaid and normalized by $\frac{\mathcal{B}(D^0 \to \pi^- e^+ \nu)}{\mathcal{B}(D^0 \to K^- e^+ \nu)} = 0.1$ from PDG [6]. The right plot shows the projection onto the U axis in linear and log scales.

In Fig. 5, we present the U distributions from data and MC for the selected $D^0 \to K^- e^+ \nu$ events with different tag modes. The comparison shows good agreement between the data and MC. Fig. 6 shows the decomposition of the U distributions from MC for all tag modes combined. The fit to the data is shown in Fig. 10. The $D^0 \to K^- e^+ \nu$ yields from various D^0 tag modes are given in Table I. The efficiencies and branching fractions are also listed in Table I for different tag modes.

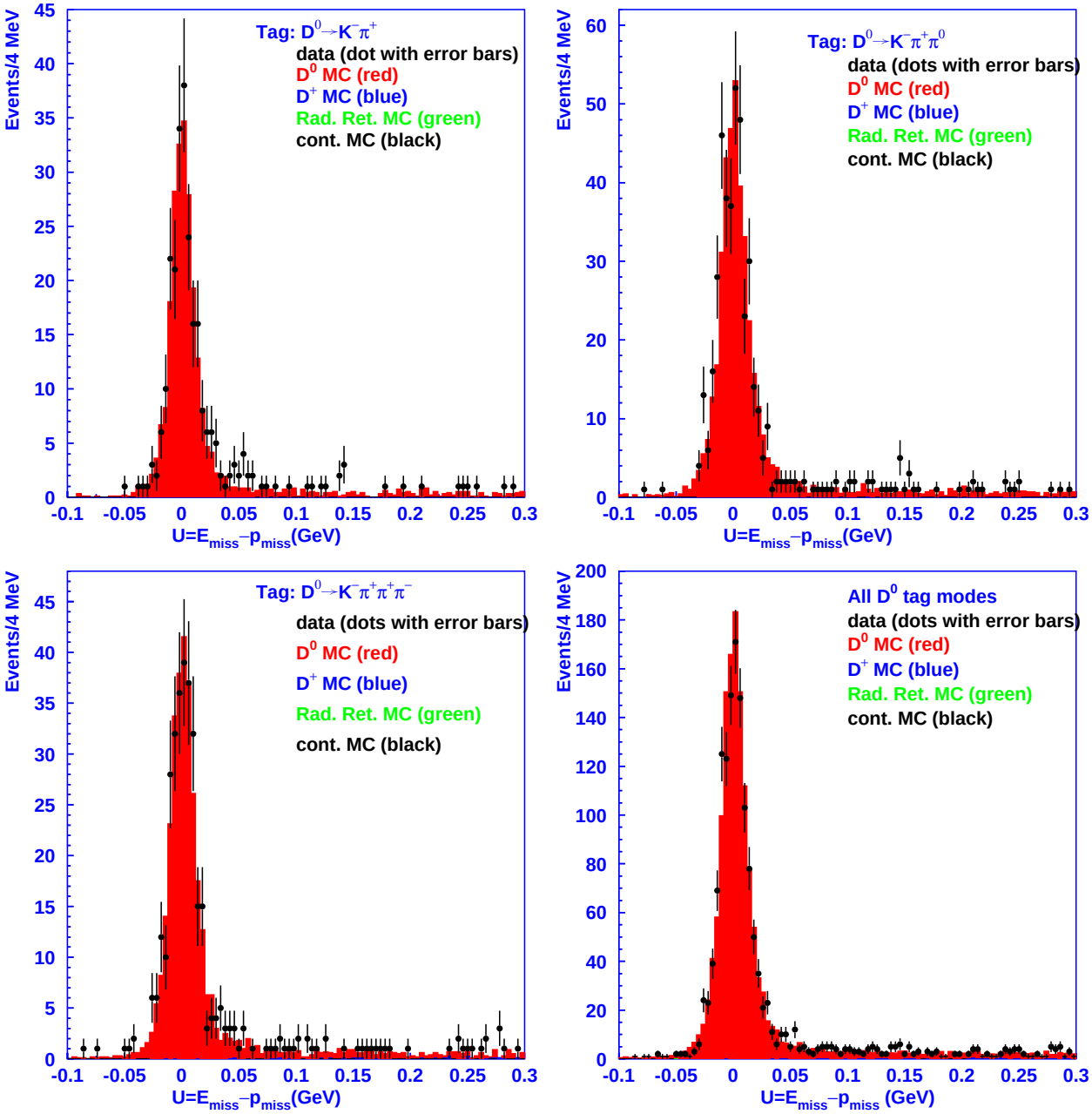

FIG. 5: Comparison of $U = E_{\rm miss} - p_{\rm miss}$ for $D^0 \to K^- e^+ \nu$ between the data and MC.

In Fig. 7, we present the U distribution from data and MC for the selected $D^0 \to \pi^- e^+ \nu$ events with all tag modes combined due to limited statistics. The comparison shows rea-

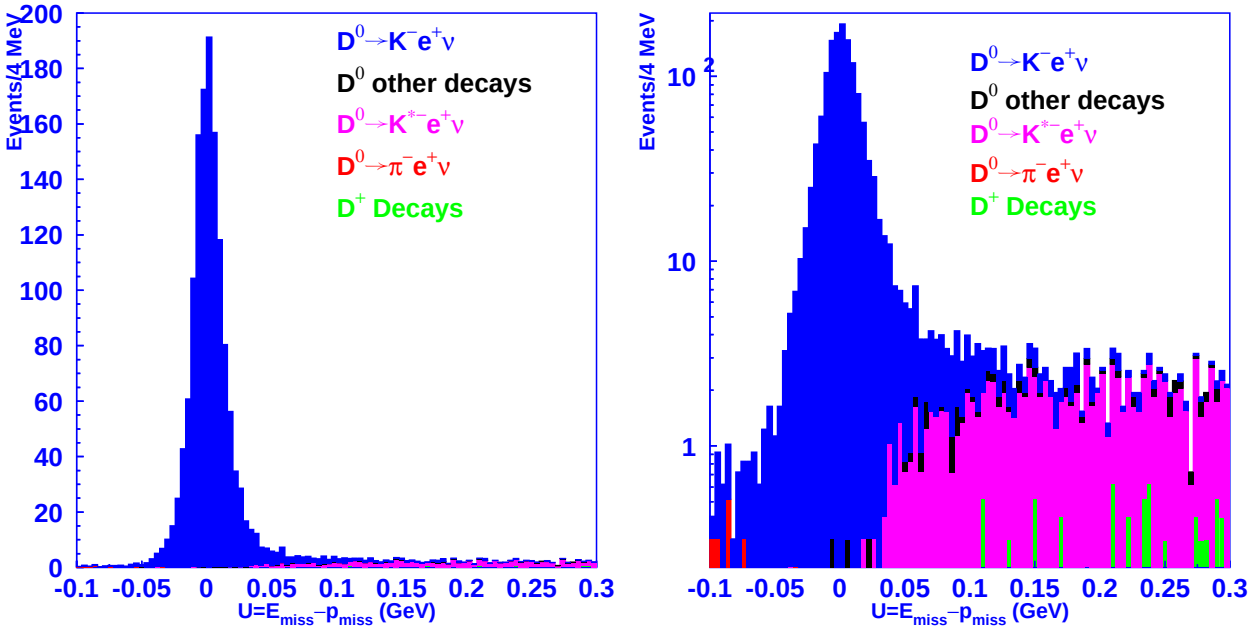

FIG. 6: Decomposition of $U = E_{\rm miss} - p_{\rm miss}$ for $D^0 \to K^- e^+ \nu$ from MC for all tag modes combined.

sonable agreement between data and MC. There is a clear excess in the $D^0 \to \pi^- e^+ \nu$ signal region (near zero) in data which is in good agreement with MC prediction. The background decomposition is also shown in Fig. 7. We fit the U distribution with a Gaussian, which corresponds to the $D^0 \to \pi^- e^+ \nu$ signal near zero, another Gaussian which corresponds to the $D^0 \to K^- e^+ \nu$ background on the right side, and a 2nd order polynomial function. The 2nd order polynomial is determined from MC simulation. The fit to the data is shown in Fig. 10. We observe 109.1±10.9 events. The signal efficiencies and branching fractions are given in Table II.

In Fig. 8, we present the comparison between the data and MC for $D^0 \to K^{*-} e^+ \nu$. The comparison shows good agreement between data and MC. The background decomposition is also shown in Fig. 8. We fit the U distribution with a Gaussian and a 2nd order polynomial determined from MC simulation. The fit to the data is shown in Fig. 10. The yields and efficiencies are given in Table II.

The comparison of the U distribution for the data and MC for $D^0 \to \rho^- e^+ \nu$ is shown in Fig. 9. The background decomposition is shown in Fig. 9. We fit the U distribution with a Gaussian which corresponds to the $D^0 \to \rho^- e^+ \nu$ signal, another Gaussian for backgrounds mainly from $D^0 \to K^{*-} e^+ \nu$, and a 2nd order polynomial function determined from MC simulation. The fit to the data is shown in Fig. 10. The yields and efficiencies are given in Table II.

To determine V_{cs} and V_{cd}, we need to study the q^2-dependent differential decay rate. Energy-momentum conservation is used to determine q^2 in the laboratory frame

$$\begin{aligned} E_W &= E_b - E_P, \\ \vec{p}_W &= -\vec{p}_D - \vec{p}_P, \\ q^2 &= E_W^2 - |\vec{p_W}|^2. \end{aligned} \tag{4}$$

Here E_W and $\vec{p}_W$ are the energy and momentum vector of the $\ell\nu$ system or the virtual W. $\vec{p}_D$

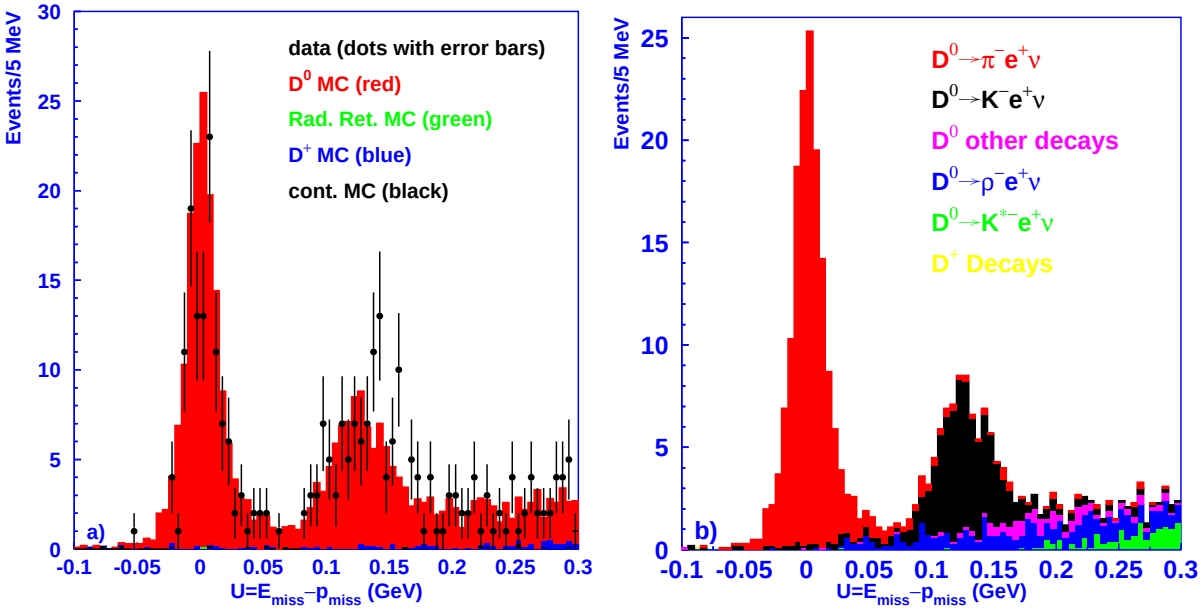

FIG. 7: $U = E_{\rm miss} - p_{\rm miss}$ for the selected $D^0 \to \pi^- e^+ \nu$ events (left), and the background components (right).

TABLE II: Efficiencies and yields for $D^0 \to \pi^- e^+ \nu$, $D^0 \to K^{*-} e^+ \nu$ and $D^0 \to \rho^- e^+ \nu$ using different tag modes.

Signal Modes	$D^0 \to \pi^- e^+ \nu$	$D^0 \to K^{*-} e^+ \nu$	$D^0 \to \rho^- e^+ \nu$
Tags	ϵ	ϵ	ϵ
$D^0 \to K^- \pi^+$	(48.06±0.30)%	(14.34±0.21)%	(18.13±0.22)%
$D^0 \to K^- \pi^+ \pi^0$	(24.93±0.26)%	(6.97±0.15)%	(8.90±0.16)%
$D^0 \to K^- \pi^+ \pi^0 \pi^0$	(12.47±0.20)%	(3.51±0.11)%	(4.52±0.12)%
$D^0 \to K^- \pi^+ \pi^+ \pi^-$	(33.28±0.29)%	(9.61±0.17)%	(11.62±0.19)%
$D^0 \to K_S \pi^+ \pi^-$	(25.77±0.27)%	(7.99±0.16)%	(9.45±0.17)%
$D^0 \to K_S \pi^+ \pi^- \pi^0$	(14.18±0.15)%	(3.95±0.11)%	(4.94±0.13)%
$D^0 \to K_S \pi^0$	(21.45±0.25)%	(6.28±0.14)%	(7.39±0.15)%
$D^0 \to \pi^- \pi^+ \pi^0$	(28.98±0.27)%	(8.83±0.17)%	(10.64±0.18)%
$D^0 \to K^- K^+$	(40.14±0.29)%	(12.33±0.19)%	(15.14±0.21)%
Yields	109.1±10.9	88.0±9.7	30.1±5.8
$\mathcal{B}(\times 10^{-3})$	(2.46±0.25)	20.69±2.28	1.89 ± 0.36

is the momentum vector of the tagging D meson. E_P and $\vec{p}_P$ are the energy and momentum vector of the hadronic system in the other D semileptonic decays.

In Fig. 11, we present q^2 distributions for $D^0 \to K^- e^+ \nu$, $D^0 \to \pi^- e^+ \nu$ and $D^0 \to K^{*-} e^+ \nu$ from data. These q^2 distributions are from data directly, without any efficiency correction. Our q^2 resolution is about 0.025 GeV^2 or smaller which is over a factor of 10 better than CLEO III which achieved a resolution of 0.4 GeV^2 [7]. This huge improvement in resolution is

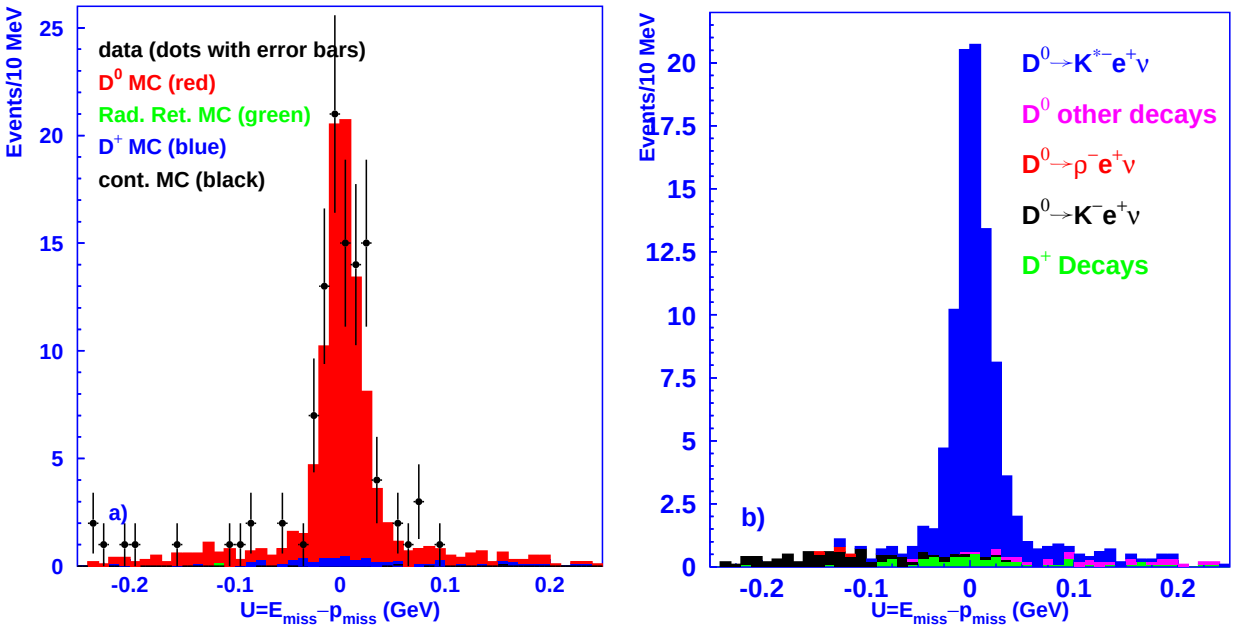

FIG. 8: U distribution for the selected $D^0 \to K^{*-}e^+\nu$ events (left) and the components of backgrounds for $D^0 \to K^{*-}e^+\nu$ (right).

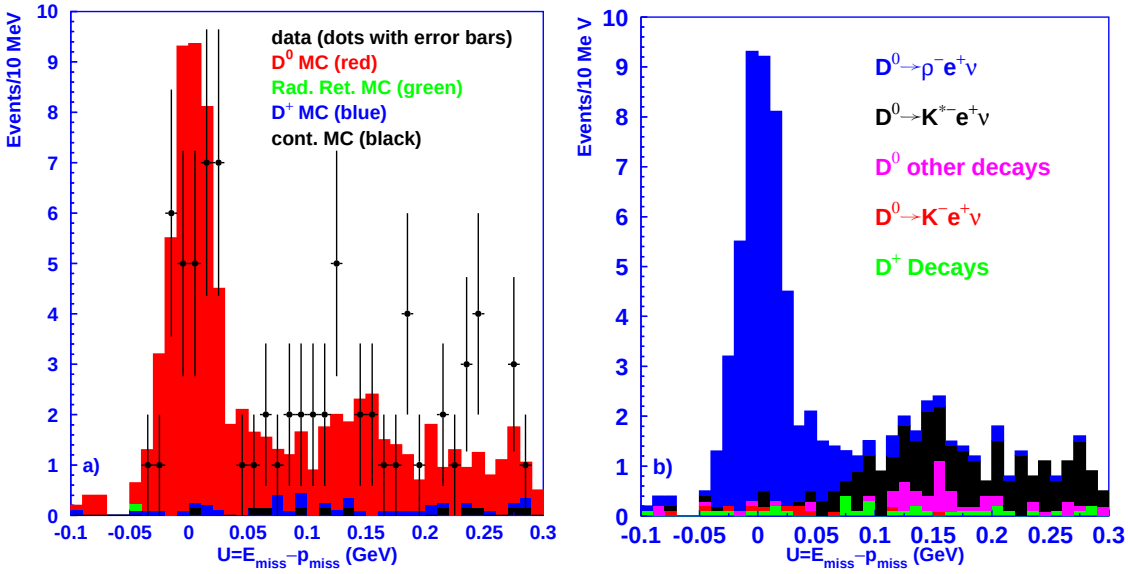

FIG. 9: U distribution for the selected $D^0 \to \rho^- e^+\nu$ events (left) and the decomposition of backgrounds (right).

due to the unique kinematics at the $\psi(3770)$ resonance. The q^2 distribution for $D^0 \to \rho^- e^+\nu$ from data is not shown due to the very limited statistics. Detailed study and measurements of form factor and CKM matrix elements will be performed with more CLEO-c data.

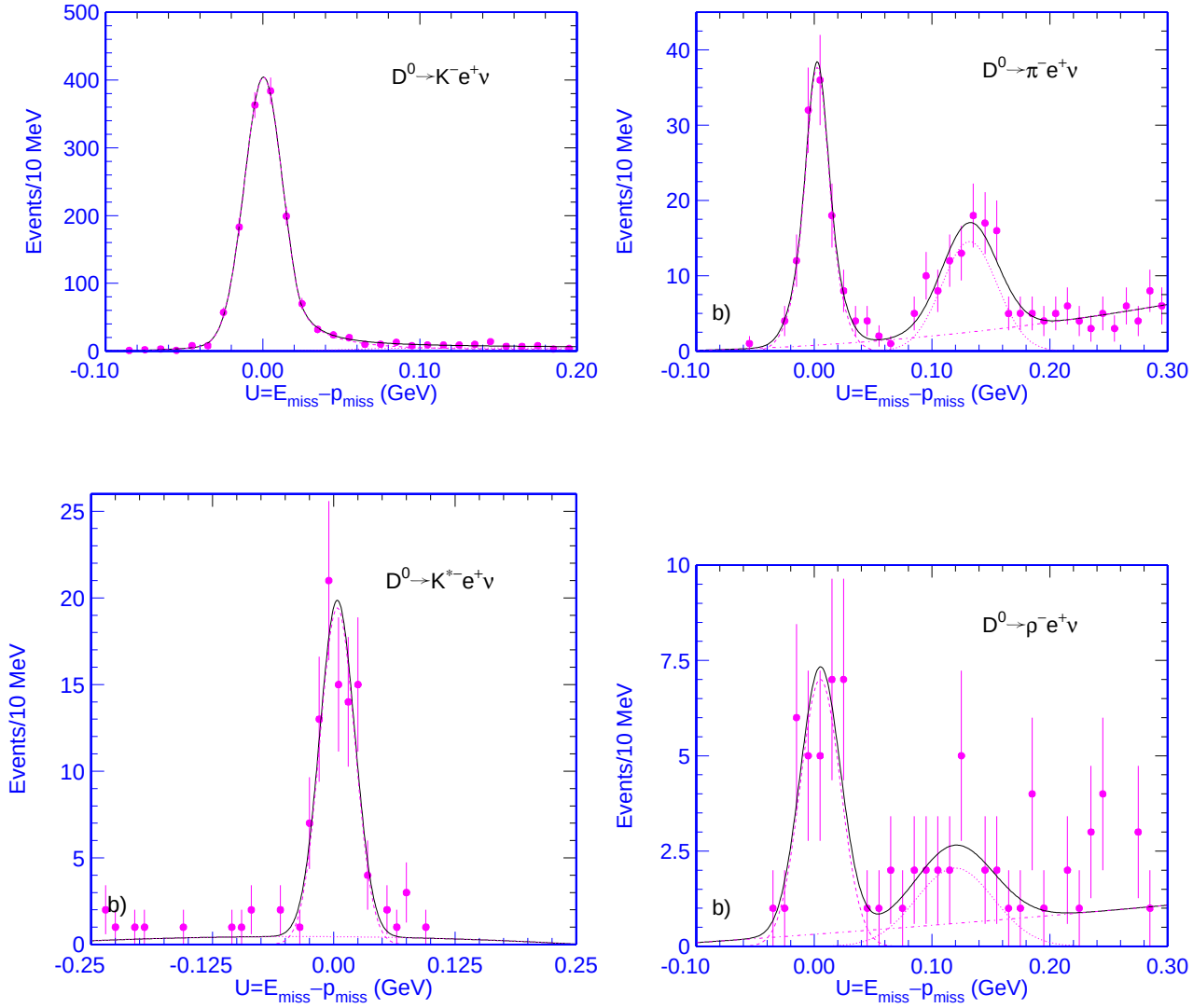

FIG. 10: Fits to $U = E_{\rm miss} - p_{\rm miss}$ distributions for $D^0 \to K^- e^+ \nu$, $\pi^- e^+ \nu$, $K^{*-} e^+ \nu$ and $\rho^- e^+ \nu$, with the other $\bar{D}^0$ fully reconstructed.

V. SYSTEMATIC UNCERTAINTIES

We have considered the following sources of systematic errors which may affect our results: charged track and π^0 finding, the veto on extra tracks, background normalization and shape, MC statistics, incomplete modeling of radiative corrections, model-dependent form factors, hadron identification, and electron identification. The contributions of these systematic errors are discussed below.

From studies of CLEO-c data and MC, the systematic error for track finding efficiency is estimated to be 3% per charged track, 4.4% per π^0 and 3% per K^0_S. The systematic errors in particle identification are 2% for electron and 1% for pion or kaon. MC statistics varies from 1% to 3%, depending on the tag modes. To test the potential effect of uncertainties in

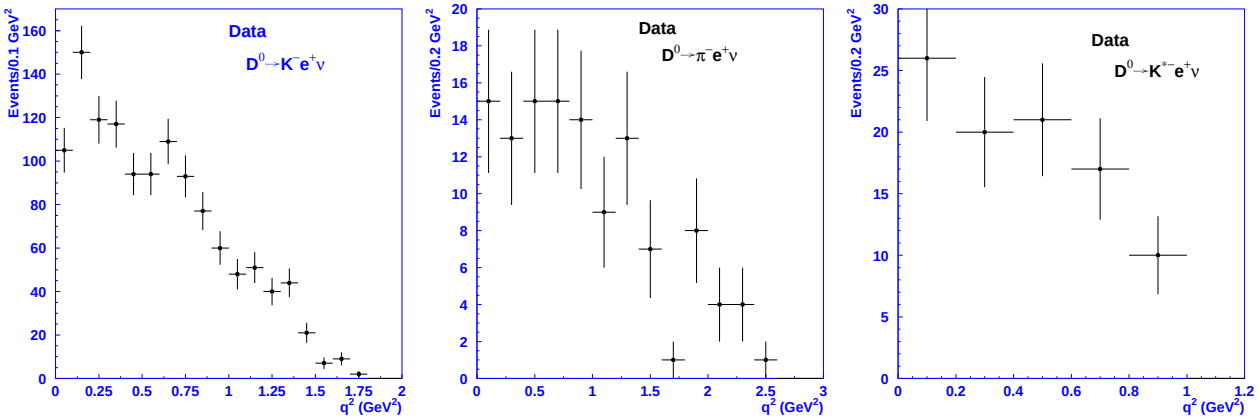

FIG. 11: Uncorrected q^2 distributions for $D^0 \to K^- e^+ \nu$, $D^0 \to \pi^- e^+ \nu$, $D^0 \to K^{*-} e^+ \nu$.

radiative corrections, we have generated signal MC with and without ISR, and have found that the efficiencies vary within 1%. Using the selected $D^0 \to K^- e^+ \nu$ events, we find 0.51% events have extra tracks in our data, 0.41% events in our MC. Therefore, we assign a 0.5% systematics uncertainty due to the veto on extra tracks. To estimate the systematics from the backgrounds, we vary the background functions by $\pm 1\sigma$, taking the correlation of parameters into account. We find the background normalization and shape contributes a systematic error of 1.1%, 3.1%, 2.9% and 5.3% for $D^0 \to K^- e^+ \nu$, $D^0 \to \pi^- e^+ \nu$, $D^0 \to K^{*-} e^+ \nu$ and $D^0 \to \rho^- e^+ \nu$, respectively. Systematic uncertainties on the reconstruction efficiencies from our current knowledge of form factors are small ($< 2\%$) due to the uniform acceptance of the CLEO-c detector over large solid angle and momentum range.

Most of these systematic errors are estimated from initial study of the first CLEO-c data. We expect these systematic errors to be reduced in the future, with more detailed study and more CLEO-c data.

In Table III, we summarize the contributions from systematic errors discussed above. The systematic errors from MC statistics is weighted with tag yields. We add these sources in quadrature to obtain the total systematic error for each decay mode.

VI. SUMMARY

In summary, we present improved measurements of exclusive D^0 semileptonic decays using the first CLEO-c data. The absolute branching fractions are listed in Table IV.

Our results for $D^0 \to K^- e^+ \nu$ and $D^0 \to K^{*-} e^+ \nu$ are consistent with those from the PDG [6]. Our $\mathcal{B}(D^0 \to \pi^- e^+ \nu)$ result is lower than that from the PDG [6]. The ratio $\frac{\mathcal{B}(D^0 \to \pi^- e^+ \nu)}{\mathcal{B}(D^0 \to K^- e^+ \nu)}$ is closer to the CLEO III result [7] of $(8.2 \pm 0.6 \pm 0.5)\%$, while lower than the PDG value [6]. The improved precision in these branching fractions is consistent with the expected performance of CLEO-c with initial data sample of 60 pb^{-1} at the $\psi(3770)$. The full integrated luminosity of $\sim$3 fb^{-1} can be expected to provide great improvement in our knowledge of a much larger set of D^0 and D^+ exclusive semileptonic branching fractions as well as decay form factors and the CKM matrix elements V_{cs} and V_{cd} [3].

We gratefully acknowledge the effort of the CESR staff in providing us with excellent luminosity and running conditions. This work was supported by the National Science Foun-

TABLE III: Systematics for four D^0 semileptonic decays (in %).

sources	$D^0 \to K^- e^+ \nu$	$D^0 \to \pi^- e^+ \nu$	$D^0 \to K^{*-} e^+ \nu$	$D^0 \to \rho^- e^+ \nu$
tracking	6	6	6	6
π^0 finding	-	-	4.4	4.4
EID	2	2	2	2
PID	1	1	1	1
extra track	0.5	0.5	0.5	0.5
MC statistics	<1	1.1	2.2	1.9
backgrounds	1.1	3.1	2.9	5.3
ISR	1	1	1	1
Form factors	< 2	< 2	< 2	5.0
Yields	1	1.9	1	2.7
Total	7.0	7.8	8.9	11.2

TABLE IV: Absolute branching fraction measurements of the exclusive D^0 semileptonic decays, in comparison with PDG [6]. The uncertaities are statistical and systematic, respectively.

Decays	$\mathcal{B}$	PDG
$D^0 \to K^- e^+ \nu$	$(3.52 \pm 0.10 \pm 0.25)\%$	$(3.58 \pm 0.18)\%$
$D^0 \to \pi^- e^+ \nu$	$(0.25 \pm 0.03 \pm 0.02)\%$	$(0.36 \pm 0.06)\%$
$D^0 \to K^{*-} e^+ \nu$	$(2.07 \pm 0.23 \pm 0.18)\%$	$(2.15 \pm 0.35)\%$
$D^0 \to \rho^- e^+ \nu$	$(0.19 \pm 0.04 \pm 0.02)\%$	none
$\frac{\mathcal{B}(D^0 \to \pi^- e^+ \nu)}{\mathcal{B}(D^0 \to K^- e^+ \nu)}$	$(7.0 \pm 0.7 \pm 0.3)\%$	$(10.1 \pm 1.8)\%$
$\frac{\mathcal{B}(D^0 \to \rho^- e^+ \nu)}{\mathcal{B}(D^0 \to K^{*-} e^+ \nu)}$	$(9.2 \pm 2.0 \pm 0.8)\%$	none

dation, the U.S. Department of Energy, the Research Corporation, and the Texas Advanced Research Program.

[1] B. Grinstein, N. Isgur and M. B. Wise, Phys. Rev. Lett. **56** (1986) 258; F. J. Gilman and R. L. Singleton, Phys. Rev. D **41** (1990) 142; K. Hagiwara, A. D. Martin and M. F. Wade, Nucl. Phys. B **327** (1989) 569.

[2] CLEO Collaboration, Y. Kubota *et al.*, Nucl. Instrum. Methods A **320**, 66 (1992); T. Hill, Nucl. Instrum. Methods A **418**, 32 (1998); D. Peterson *et al.*, Nucl. Instrum. Methods A **478**, 142 (2002); M. Artuso *et al.*, Nucl. Instrum. Methods A **502**, 91 (2003).

[3] CLEO-c Collaboration, CLNS-01/1742.

[4] CLEO-c Collaboration, CLEO CONF 04-10, ICHEP04 ABS11-0775.

[5] ARGUS Collaboration, H. Albrecht *et al.*, Phys. Lett. B **241** (1990) 278.

[6] Particle Data Group, K. Hagiwara *et al.*, Phys. Rev. D **66**, 010001 (2002).

[7] CLEO Collaboration, G.S. Huang *et al.*, CLNS 04/1876, CLEO 04-06, CLEO CONF 04-14 and ICHEP04 ABS11-0780. Submitted to Phys. Rev. Lett.